Oncogenic HJURP is driven by P53/ E2F1/FOXM1-axis regulated enhancer and potentiates TNBC proliferation and invasion

yunlu jia (jiayunlu@zju.edu.cn)
Zhejiang University School of Medicine First Affiliated Hospital

Yongxia Chen
Zhejiang University School of Medicine Sir Run Run Shaw Hospital

Ming Chen
Zhejiang University School of Medicine First Affiliated Hospital

Jianbiao Zhou
National University of Singapore

Wee-Joo Chng
National University of Singapore Yong Loo Lin School of Medicine

Mixue Xie
Zhejiang University School of Medicine

Qi Jiang
Zhejiang University School of Medicine

Hanchu Xiong
Zhejiang University School of Medicine

Jian Ruan
Zhejiang University School of Medicine

Linbo Wang
Zhejiang University School of Medicine

Peng Shen
Zhejiang University School of Medicine

Research Article

Keywords: HJURP, Enhancers, P53, E2F1, TNBC

Posted Date: January 19th, 2023

DOI: https://doi.org/10.21203/rs.3.rs-2465454/v1

Abstract

Triple-negative breast cancer (TNBC) is the most aggressive subtype of breast cancer with poor outcomes and lacks effective targeted therapies. We utilized the epigenomic landscape, TCGA database and clinical samples to show the activation of *HJURP* in TNBC, which is associated with poor prognosis, metastasis, and advanced stage. RNA-seq analysis of *HJURP* silencing induced malignant phenotypes-related transcriptional signatures of TNBC. Specifically, knock-down of *HJURP* suppressed cell proliferation, migration, invasion, EMT progress, and induced apoptosis of TNBC. Analysis of publicly available data sets revealed that *HJURP* is elevated in mutP53 vs. wtP53 breast cancer cells. Inactivation of wild type P53, by loss or mutation of wtP53, increased *HJURP* expression, whereas accumulation of wild-type P53 reduced *HJURP* promoter activity and *HJURP* transcription. We found the activation of *HJURP* in TNBC was driven by the mutant P53-regulated enhancer instead of genetic alteration. *P53* positively regulated the expression of transcription factor *FOXM1* and *E2F1*, and the FOXM1/E2F1/H3K27ac complex preferentially occupied the *HJURP*-enhancer and regulated *HJURP* transcription by binding to the active elements. CRISPR interference of enhancer structure or specific disruption of enhancer complex inhibited *HJURP* transcription and phenocopied *HJURP* silencing, leading to impaired *E2F1*, *FOXM1* and *H3K27ac* binding affinity. Consistent with this result, knock-down of FOXM1 or E2F1 reduced *HJURP* expression in TNBC cells containing mutant alleles of *P53* gene. Lastly, we uncovered marked decreases in survival of breast cancer patients expressing high *HJURP* levels carrying wtP53. Our findings identify enhancer-driven *HJURP* as a molecular bypass that suppresses the anti-proliferative and pro-apoptotic effects exerted by wtP53. Targeting *HJURP* allows for effective suppression of tumor invasion and attenuating metastasis in P53-mutant TNBC.

Introduction

Breast cancer is the leading cause of cancer death among women worldwide, a heterogeneous disease of distinct genetic, epigenetic, and transcriptomic alterations[1]. Triple-negative breast cancers (TNBCs) accounts for up to 15% of all breast cancers and are more aggressive than tumors of other molecular subtypes, in terms of biology, molecular features and response to treatment[2]. Besides chemotherapy, there are few therapeutic options available to TNBCs. Due to a lack of validated therapeutic targets, patients with TNBCs have the disadvantage of not benefiting from targeted therapies. Besides, the deregulation of breast cancer epigenome in different molecular subtypes that results in various phenotypic outcomes remains incompletely unravelled.

Enhancers are DNA regulatory elements that are key regulators of lineage-specifying genes. Enhancers are defined by certain histone modifications (H3K27ac, H3K4me1) and bound by chromatin-modifying transcription factors (such as BRD4, CDK7 and p300)[3]. Enhancer malfunction during carcinogenesis is observed in various tumor types. Cancer cells are dependent on the robust transcription levels from specific enhancers and enhancer dysregulation could be targeted for cancer therapy. Epigenomic profiling has been done in various solid tumors for identifying subgroup-specific enhancer-driven genes[5,6]. *P53* is

a crucial tumour suppressor and typically induces anti-proliferative function to a host of diverse stresses, such as DNA damage, hypoxia, genome instability, nutrient starvation, and oxidative stress[7]. Inactivation or mutation of *P53* is a common event during cancer development. P53 mutations are seen in 18–25% of primary breast cancers and occur more frequently in TNBC (80%). P53 mutation results in inactivating of P53 function and acquires new oncogenic properties (gain-of-function, GOF), which actively promotes tumor metastasis [8–10]. Recent studies have demonstrated that P53-dependent binding activities occur predominantly within *cis*-regulatory elements, and most P53-bound enhancers are located within inaccessible chromatin regions[11,12]. TNBCs present few highly recurrently driver alterations, except for being enriched in mutations of tumor suppressor genes such as INPP4B, PTEN, and P53, a situation that has limited the development of targeted therapies. Therefore, there is an urgent need to develop new therapeutic targeting approaches for P53-mutated TNBC. Novel agents against aberrant P53 signaling and P53-target genes were considered as a novel approach to prompting the implementation of biomarker-driven therapeutic approaches.

In this study, we aimed to map the unique active cis-regulatory landscape in TNBC based on H3K27ac chromatin immunoprecipitation sequencing (ChIP-Seq) data and global gene expression. We identified corresponding target genes of TNBC-specific enhancers, including the novel enhancer-associated gene - Holliday Junction Recognition Protein (*HJURP*, also known as *hFLEG1*). The critical function of *HJURP* in breast cancer proliferation and its clinical relevance has been determined in this study. Phenotypically, downregulation of *HJURP* resulted in decreased tumor growth, invasion and migration. *HJURP* is a histone assembly factor reported to function at centromeres and interact with *CENP-A*[13]. *HJURP* localization and licensing to stabilizes *CENP-A* at centromeres, plays an established role in cell cycle progression [14]. The oncogenic function of *HJURP* has been reported in the progression of various solid tumors, and increased *HJURP* expression is correlated with unfavourable prognosis of patients with breast cancer[15,16]. We previously reported the oncogenic role of superenhancer-driven *HJURP* in myeloma and the novel mechanism by which it was regulated to offer new insights into myeloma biology[17]. Recently research revealed that *HJURP* is transcriptionally activated in *P53*-null cancer cells in response to aneuploidy[18]. P*53* repressed the transcription of murine *Hjurp* and *Cenpa* via the putative CDE/CHR elements within the promoter regions. However, further research is required to clarify the precise roles and molecular mechanisms of HJURP in the pathogenesis of TNBC. Here, examination of transcriptional drivers for epigenomic subtypes uncovered TNBC samples with a new enhancer formation downstream the transcription start site (TSS) of *HJURP* gene. Profiling of *HJURP* expression levels in human breast tumors revealed the aberrant activation of *HJURP* in TNBC that frequently harbor *P53* mutations, which are attributed to the active enhancer. We seek to identify the functional relevance of enhancer-associated *HJURP* and understand the regulatory association between *HJURP* and *P53* of TNBC.

Materials And Methods

Cell lines and Reagents

All of the cell lines used in this study were acquired from American Type Culture Collection (ATCC, Rockville, MD, USA), and were grown in the recommended culture media. Briefly, RPMI 1640 supplemented with 10% fetal bovine serum (FBS) was used for BT-549, MCF-7, ZR-75-1, SK-BR-3, HCC1937, Hs578T, T-47D, MDA-MB-231, MCF-10A and NHFB. Pifithrina-α (Pthα) was purchased from Biomol (Plymouth Meeting, PA). MDM2 Inhibitor Nutlin-3a (SML0580) was purchased from Sigma-Aldrich (Millipore Sigma, US). All antibodies used are shown in supplementary materials and methods.

Crispr-dcas9 For Disruption Of Hjurp Enhancer Region

CRISPR guide RNAs were designed by the CRISPR direct design tool (https://crispr.dbcls.jp/), and then synthesized and subcloned into the lent guide-blasticidin plasmid and infected into dCas9-KRAB stable-expressing cells. The CRISPR (Addgene, Plasmid #71236) and gRNA with fluorescent GFP reporter vectors (Addgene, Plasmid#70183) were gifts from Dr. Takaomi Sanda. Following nucleofection, cells were allowed to grow in RPMI 1640 supplemented with 10% FBS. Established colonies were screened by PCR for the region encompassing the two CRISPR target sites in HJURP enhancer region, using primers with the sequences 5'- CCAACCCGGTAAGCCGGAGGCAT-3' and 5'- CCGGTAAGCCGGAGGCATGTGAG – 3'

Tissue Microarray Immunohistochemistry

Tissue microarrays containing paired of human breast tumor specimens and normal breast tissue specimens were purchased from TBS-bio (Xian, China). Slides were stained using the GTvisionIII Immunohistochemical Assay Kit (HRP/DAB, rabbit/mouse-general, two-step, GK500710, Gene Tech, Shanghai, China) according to the manufacturer's protocol. Immunohistochemical assays were performed using the following antibodies: HJURP ((Sigma-Aldrich, HPA008436, dilution 1:250). Images were acquired by polarized light microscopy.

Rna-seq Analysis

RNA-seq was performed to investigate the mRNA expression profiles after HJURP silencing in BT-549 and MDA-MB-231 cells, and *HJURP* overexpression in MCF-7 cells. Three biological replicates were carried out at the LC-bio (Hangzhou, China) using HiSeq 2500 (Illumina, USA). Indexed samples were sequenced on an Illumina HiSeq 2500 in a single read mode. Differential gene expression was calculated applying the DESeq2 software (version 1.2.10). Fold change > 1.5 were set as the cut-off values to select differentially expressed genes and gene set enrichment analysis (GSEA) analysis was applied for pathway enrichment with $P < 0.05$.

chromatin Immunoprecipitation (Chip) Assay Coupled With Quantitative Pcr

ChIP was performed using the ChIP Assay kit (SimpleChIP® Enzymatic Chromatin IP Kit (Magnetic Beads), Cell Signaling Technology, #9003). Chromatin was used for immunoprecipitation with anti-H3K27ac, anti-P53, anti-BRD4, anti-RNA polymerase II, and a normal rabbitIgG antibody. ChIP-enriched DNA was measured using qRT-PCR, and the primers for detecting the expected DNA binding sequence were designed as follows: E1, forward 5-TCCCGTACGGAGGCCGAATGGC-3 and reverse 5-CTTTTCGGACGACCTGGAG-3; E2, forward 5-TCCCGCTTACCCTGTGGCGTCTCGT-3 and reverse 5-AAACACGAGACGCCACAGGGTAAGC-3. E3, forward 5- TCCCGAGGCGACGTCTCTGGCGCAA-3 and reverse 5- AAACTTGCGCCAGAGACGTCGCCTC-3; E4, forward 5-TCCCGGGAGAAGCCGGGCACTGATT-3 and reverse 5- AAACAATCAGTGCCCGGCTTCTCCC-3. After 32 to 35 cycles of amplification, PCR products were run on a 1.5% agarose gel and analyzed by ethidium bromide staining.

Mammary Orthotopic Tumor Xenograft Assays

Animals were housed in a specific pathogen-free facility (Zhejiang University Animal Care Services), with ventilated cages and sterilized food and water supply. All procedures with mice were approved by the Zhejiang University Animal Care Committee. Control shRNA, *HJURP* shRNA cells were grown to 70 to 85% confluence before trypsinization and counting. For xenograft assays, 1.0×10^6 cells were injected into the right thoracic mammary fat pads in a volume of 50 μl of 50% Matrigel using a hypodermic syringe. At end points of 4 weeks mice were sacrificed and primary tumor weight and volume were recorded. The primary tumors from each mouse were used for histological staining analysis. Samples were fixed in formalin and embedded in paraffin, and 5 μm sections were stained with HJURP and KI67-antibodies. Stained sections were scanned using the Aperio CS digital slide scanner and analyzed with ImageScope software.

Statistics Analysis

Data are presented as the mean ± standard error of the mean (SEM) from three independent experiments. The Student's t-test was employed to compare the differences between two groups or among more than two groups. Fisher's exact test was applied to analyze the relationship between clinicopathological features and *HJURP* expression. Pearson's correlation was performed to analyze the link between *HJURP* and *E2F1, FOXM1* expression. $P < 0.05$ was considered statistically significant. All data were analyzed using GraphPad Prism 7.0.

Results

Elevation of HJURP in breast cancer subtypes carrying frequent P53 mutations

We first aimed to stratify the data of RNA-Sequencing available from The Cancer Genome Atlas (TCGA) according to four main molecular subtypes of breast cancer: Luminal A, Luminal B, Triple-negative/basal-like, HER2-enriched. Correlation between *HJURP* expression levels and gene copy numbers and specific

oncogenic mutations was also detected in the TCGA and Gene Expression Omnibus (GEO) datasets. P53 mutational spectrum and the prognostic implications indeed are subtype-specific. Consistently with the amplified frequency of P53 mutations in HER2 and TNBC subtypes, higher expression of *HJURP* was detected in triple-negative/basal-like and HER2-enriched subtypes compared to luminal tumors (Fig. 1A, Supplementary Fig. 1A-C). Overall mutation frequency in the breast cancer cohorts (PanCancer Altas and METABRIC) also indicated p53 mutation as the most common alteration in the HJURP-altered group (Fig. 1B). Expression of *HJURP* was presented to be positively correlated with proliferation marker as *MKI67, PCNA, BRCA1* and *BRCA2*, and negatively correlated with *ER* and *PR* (Fig. 1C, Table 1). Our analysis found that *HJURP* expression was enriched in breast tumors carrying P53 mutations in TCGA and GEO data sets (Fig. 1D, Supplementary Fig. 1D). Interestingly, this effect was most substantial in the luminal-type tumors, suggesting a subtype-related mechanism contributing to *HJURP* activation and P53 mutagenesis (Fig. 1E). Furthermore, *HJURP* expression is also elevated in various mutp53 human tumors types, including the lung, bladder, and stomach tumors (Supplementary Fig. 1E). Besides, *HJURP* was also highly-expressed in TNBC compared with normal breast tissue and non-TNBC breast cancers, and the elevation of *HJURP* expression occurred in late-stage breast cancers (Supplementary Fig. 1F, G).

We next sought to detect *HJURP* expression in a selected panel of mutp53 and wtp53 breast cancer cell lines. Consistent with our findings, up-regulation of *HJURP* transcript and protein was clearly examined in breast cancer cell lines carrying mutp53 (Fig. 1F). Immunofluorescence assay further confirmed the much higher expression of HJURP in mutp53 MDA-MB-231 and BT-549 cells than that of wtp53 MCF-7 cells, and HJURP mainly localized to the cellular nuclear (Fig. 1G, H). To evaluate associations between HJURP protein content and breast cancer patient outcomes, we stained and analyzed a human tissue microarray (TMA) with annotated P53 mutation status, which consisting of primary breast tumor specimens and normal breast tissue, and for which molecular subtypes were available. Examples of HJURP-stained images from cases displaying abundant (HJURP high) or reduced HJURP staining (HJURP-low) are shown in Fig. 1I. Analysis of the TCGA cohort revealed a significant association of *HJURP* overexpression with tumor patient age, tumor grade, tumor size, ER/PR/HER2 status and lymph node metastasis (Table 2). Collectively, HJURP is highly expressed in human breast cancer subtypes with frequent P53 mutations, with certain clinical characteristics of breast cancer patients.

Inhibition of HJURP impaired cell growth and sensitized cells to chemotherapy regimens in TNBC carrying mutP53

We next utilized a loss- and gain-of-function strategy to elucidate the function of *HJURP* in regulating breast cancer cell biology. BT-549 and MDA-MB-231 cells carrying mutP53 were selected for *HJURP* shRNA knock-down experiments (Fig. 2A, B). Silencing of *HJURP* in BT-549 and MDA-MB-231 cells suppressed cell growth over time, compared with lentivirus carrying control shRNA transduced cells (Fig. 2C). We next determined the effects of *HJURP* silencing on cell growth by clonogenic cell survival assay. Deletion of *HJURP* reduced colony formation in both BT-549 and MDA-MB-231 cells (Fig. 2D). The group of *HJURP* knock-down showed a significantly higher apoptosis rate than the control. Expression levels of apoptosis markers as cleaved-PARP, cleaved-caspase 3 and 7 were increased in the *HJURP*

silencing group compared to the control group (Fig. 2E, F). The function of *HJURP* in regulating cellular migration and invasion was explored using a Matrigel-coated Transwell assay. We found that knock-down of *HJURP* significantly reduced the ability of TNBC to migrate and invade through Matrigel (Fig. 2G, H). Cancer cells undergoing epithelial-mesenchymal transition (EMT) acquire a cancer stem-like phenotypes and metastatic traits associated with malignant behaviours. Here we found that *HJURP* is a major inducer of EMT progress. *HJURP* ablation prevented EMT and maintained an epithelial morphology of TNBCs (Fig. 2I). These results showed that *HJURP* silencing not only reduced cancer cell viability but also inhibited the metastatic capacity and EMT, which is crucial for an effective treatment strategy.

We next determined the role of *HJURP* on tumor proliferation using transplanted tumor mouse models. The tumor formation and growth of transplanted tumors were monitored for four weeks and we found that knockdown of *HJURP* led to impaired growth ability of MDA-MB231-engrafted tumors (Fig. 2J, Supplementary Fig. 2A). The tumor weights of Lenti-shHJURP-group were significantly lower than the control group (Fig. 2K). Moreover, we performed HJURP, and KI67 staining of randomly selected mouse tumors, and decreased KI67 and HJURP expression was detected in shHJURP-group (Fig. 2L). Altogether, these data indicate that *HJURP* inhibition suppresses the proliferation of MDA-MB231–engrafted tumours.

As cancer cells carrying mutp53 strongly rely on P53 GOF for survival, we determined whether silencing of *HJURP* affected the mutp53 expression level. We found that HJURP silencing by specific siRNA exerted a limited effect on mutP53 expression level in BT-549 and MDA-MB-231 cells (Supplementary Fig. 2B). Recent work has indicated P53 as a predictor of chemotherapy response in cancer patients, and P53-positive TNBC tend to more sensitive to chemotherapy. To test the effect of HJURP loss in chemotherapy responsiveness of TNBC carrying mutP53, we knocked down HJURP in BT-549 and MDA-MB-231 cells using siRNA and measured the cell survival upon Adriamycin (DOX), Paclitaxel (PTX) or Fluorouracil (5-FU) treatment. We found that the cells transfected with HJURP siRNA had decreased cell viability upon chemotherapy regimens treatment (Fig. 2M). These attributes are accompanied by a change in cell aggressive basal-like morphology (Fig. 2N, Supplementary Fig. 2C). Taken together, these data demonstrate loss-function of *HJURP* is associated with decreased cell growth, induced cell apoptosis and enhanced sensitivity to chemotherapy regimens in TNBC carrying mutp53.

HJURP **overexpression bypassed P53-mediated growth arrest in wtp53 breast cancer cell**

The functional effects of *HJURP* overexpression were investigated in wtp53 breast cancer cell lines MCF-7 and ZR-75-1 using in vitro assays. Previously, RT-qPCR analysis among a list of breast cancer cell lines illustrated that MCF-7 and ZR-75-1 cells expressed *HJURP* at relatively low levels. Overexpression of *HJURP* in MCF-7 and ZR-75-1 cells after lentivirus vector infection was confirmed by RT-qPCR and western blot analysis, and the expression level of P53 showed no obvious difference (Fig. 3A). We next use cellular functional assays to reveal that *HJURP* overexpression alone exerted a limited effect on cell migration and invasion ability (Fig. 3B, C). *HJURP* overexpression caused increased cell proliferation and decreased cell apoptosis in ZR-75-1 and MCF-7 cells (Fig. 3D, E). Considering the essential tumor-

suppressive function of wtp53 in MCF-7 and ZR-75-1, we used a small-molecule inhibitor of P53-mediated transcription, pifithrin α (Pthα), to test the role of wtp53 in mediating *HJURP* function and whether *HJURP* could bypass either P53-mediated growth arrest or apoptosis (Fig. 3F). Colony formation was observed in the absence of Pthα, or transduced into a provirus containing *HJURP* or a control provirus. In cells with P53 inhibition (Pthα-treatment group), *HJURP* overexpression rescued proliferation of MCF-7 and ZR-75-1 cells (Fig. 3G). It was concluded that wtp53 plays a central role in mediating growth arrest of wtp53 breast cancer cell, and *HJURP* was capable of bypassing wtp53 activity as a negative regulator of cell proliferation, when added as an independent factor.

Identification of gene expression signatures related to HJURP induction in breast cancer

To decipher the underlying mechanism of *HJURP* as they pertain to breast cancer cell proliferation and metastasis, we performed whole transcriptome RNA-seq analysis using BT-549 and MDA-MB-231 cells with *HJURP* inhibition or MCF-7 cells with *HJURP* overexpression. As shown in the volcano plot, we identified a total of 2456 HJURP silencing-related genes in BT-549 cells, with 1111 upregulated and 1345 downregulated genes in the HJURP deletion group compared to the control group. Besides, we identified 257 and 519 genes that were significantly up- or downregulated, respectively between the MDA-MB-231-silencing and control group (Fig. 4A). The expression levels of 86 and 115 genes were positively and negatively correlated with *HJURP* overexpression in MCF-7 cells, respectively (Fig. 4B). Among these genes potentially regulated by the *HJURP*, most were involved in certain signalling pathways, physiologic regulation, and cell growth process (Fig. 4C, D). To further narrow down transcripts related to cancer progression, upregulated or downregulated genes with at least a 1.5-fold change with HJURP overexpression or inhibition were selected The expression of several oncogenes, including *GLO1, E2F7, SPARC, GSTO1, BSCL2, GSKIP* and *FTH1*, was positively regulated by *HJURP* (Fig. 4E), and the expression of several tumor suppressor genes, as *p21, TP63* and *TP53I3*, was negatively regulated by *HJURP* (Fig. 4F). Together, these data indicated that multiple tumor-related genes are involved in *HJURP*-driven breast cancer progression.

MDA-MB-231 and BT-549 cells carry mutations in P53, and we observed that mutp53 expression was down-regulated with *HJURP* inhibition. Pathway enrichment analysis demonstrated P53 signalling pathway was induced upon HJURP silencing in BT-549 cells (Fig. 4C). Then, gene set enrichment analysis (GSEA) revealed that *HJURP* primarily affected the P53 signaling pathway, glycolysis, the G_2/M checkpoint and E2F targeting (Data not shown here). Since several studies have identified a potential relationship between *HJURP* and P53, we attempted to investigate HJURP's effect on P53. We analysed breast cancer data sets (METABRIC and TCGA) to examined whether *HJURP* expression correlated with P53-induced or repressed genes. *HJURP* expression was positively correlated with most of P53-repressed genes (*CCNB1, CDC25C, CDK1* and *BIRC5*) but not with P53-induced genes (*APAF1, CDKN1A, MYOC, BBC3*) (Fig. 4G, H). The mRNA levels of selected P53-repressed genes (*CDKN1A, BAK1, BLCAP, FOS, TOB1*) in the P53 signalling pathway were consistently affected by *HJURP* in breast cancer cells, which was confirmed by qRT-PCR analyses (Fig. 4I). Taken together, the above results suggested that *HJURP* is

a P53-response target gene and probably exerts its biological function through the inactivate P53 pathway.

Genome editing of enhancer region affected HJURP transcription

We systematically profiled regulatory landscapes in a series of TNBC (MDA-MB-231, CAL-51, BT-549, SUM 149T, SUM 159T and MDA-MB-436), non-TNBC (MCF-7, T-47D, AU565 and SK-BR-3) and normal human mammary epithelial cell (MCF-10A). Notably, significantly elevated H3K27ac signals were found at the proximal regions within *HJURP* coding sites in all TNBC samples (chromatin region: chr2:234,762,042–234,764,060). In contrast, only background level signals were present in non-TNBC cell lines and MCF-10A (Fig. 5A, Supplementary Fig. 3A). Increased enrichment of MED1, and P53-related transcription factors as E2F1, FOXM1 signals were overlapped with H3K27ac-enriched enhancer region. In addition, high-throughput measure by DNase-Seq mapped a DHS site within the cis-regulatory element, which is necessary for the binding of proteins such as transcription factors (Fig. 5B). These findings indicated that the generation of new enhancer and the aberrant activation of HJURP is specific to TNBC. Enhancers are bound by aberrant high levels of transcription factor, including CDK7 and the bromodomain and extra-terminal domain (BET) protein family, and drive cell type-specific gene expression programs. Downregulation of *HJURP* upon a specific inhibitor targeting CDK7 (THZ1) treatment was determined by qRT-PCR and immunoblot in a dose-dependent manner (Fig. 5C, D). As non-TNBC cells show no prominent enhancer activity and HJURP overexpression, we observed no significant decreased of *HJURP* expression when ZR-75-1 and MCF-7 cells were treated with THZ1 for 24 hours (Data not shown here). Similarly, JQ1, a small-molecule inhibitor blocking BRD4 binding to active enhancer elements, leading to diminished the mRNA levels of *HJURP* (Fig. 5E, Supplementary Fig. 3B, C), and consistent with published datasets (GSE63584 and GSE65201) (Supplementary Fig. 3D). Knock-down of BRD4 also affected HJURP expression (Fig. 5F). In DMSO-treated BT-549 and MDA-MB-231 cells, ChIP-qPCR data showed the presence of the typical enhancer markers, H3K27ac at E1-E4 within the *HJURP* enhancer region After JQ1 (400 nM) or THZ1 (125 nM) treatment for 24 h, H3K27ac occupancy at the four randomly selected enhancer regions was examined. H3K27ac marks at all the four sites were noticeably reduced. The suppressive effect of THZ1 and JQ1 on HJURP expression partial contributed to the decreased abundance of H3K27ac mark on the enhancer chromatin (Supplementary Fig. 5E). The ability of enhancer to regulate luciferase activities was then tested. Two loci within enhancer region (pGL3-Enhancer_1 and pGL3-Enhancer_2) and a negative control named pGL3-basic outside enhancer site were constructed. We observed that the enhancer-transfected group showed significantly increased luciferase activity compared to the corresponding control, and the THZ1 or JQ1 treatment group presented decreased luciferase activity (Fig. 5G). Together, these results indicated that *HJURP* transcription was sensitive to transcriptional inhibition targeting specific enhancer.

We then employed CRISPR interference (CRISPRi) system by transgenic expression of doxycycline (Dox) inducible dCas9-KRAB, and single-guided RNAs (sgRNAs) were designed to target the active enhancer element (Fig. 5H, Supplementary Fig. 3F). RNA-guided epigenome editing reduced HJURP expression, showing that enhancer could positively regulate HJURP transcription (Fig. 5H). As expected, we observed

that the reduction of the enrichment of H3K27ac signals within the enhancer genomic locus upon CRISPRi-mediated inactivation (Fig. 5I). Remarkedly, induced inactivation of the HJURP-enhancer led to a significant decrease in cell survival (Fig. 5J). These findings indicated that enhancer-mediated epigenetic programme contributed to *HJURP* activation in TNBC and is important for the malignant function of *HJURP* gene.

P53 regulated enhancer activity to shape HJURP transcription associated with E2F1 and FOXM1

We next tested whether *P53* regulate *HJURP* expression in mutp53 or wtp53 breast cancer cells. Silencing of *P53* using small interfering RNA (siRNA) promoted the expression of *HJURP* in wtp53 breast cancer cell lines (MCF-7 and ZR-75-1) (Fig. 6A). The small molecule Nutlin-3a inhibits the interaction between P53 and MDM2, to specifically restore P53 activity and represents an attractive approach for cancer therapy. To ensure proper pathway activation as well as RNA and protein accumulation of Nutlin-3a, P53 wild-type cancer cell lines MCF-7 and ZR-75-1 were cultured with Nutlin-3a or DMSO vehicle (untreated control) for 24 h treatment time. The expression level of MDM2, p21, and P53 was up-regulated in response to Nutlin-3a treatment. Accumulation of P53 protein resulted in decreased levels of endogenous HJURP protein in wtp53 breast cancer cells, but not in mutp53 MDA-MB-231 cells (Fig. 6B, C, Supplementary 4A). The changes in endogenous HJURP protein levels observed by immunoblotting following P53 expression correlate with the changes observed by RNA-seq for endogenous P53. P53-reactivating drugs RITA and 5-Fluorouracil (5-FU) induce its accumulation in tumor cells, with decreased expression of HJURP in breast cancer cells (Fig. 6D, E). We also assessed the effect of p53 status on HJURP gene expression in the HCT116 human colorectal cancer cell line. The HCT116 wild-type (wt), HCT116 p53+/+, and HCT116 p53-/- were employed, covering three different P53 variations. HJURP was found to be more strongly induced in HCT116 wt and HCT116 p53+/+ compared to other cell lines (Supplementary 4B). RNA-seq data presented that P53-reactivating drugs RITA induces HJURP accumulation in HCT116 parental cell but not in HCT116 P53-null cell (Supplementary 4C). We then measured enhancer luciferase activity in the presence and absence of wtP53. Induction of wtp53 (Nutlin-3a treatment group) repressed the − 5 kb HJURP enhancer activity in both MCF-7 and ZR-75-1 cells (Fig. 6F). ChIP-qPCR data showed the presence of typical enhancer markers in the HJURP enhancer region. After Nutlin-3a treatment at 20 nM for 48 h, the H3K27ac, BRD4, and RNA polymerase II occupancy at the four selected regions within the HJURP enhancer was examined, signals of active enhancer markers were noticeably decreased. These data suggested that Nutlin-3a treatment contributed to the disruption of the HJURP-enhancer in wtp53 breast cancer cells (Fig. 6G). To determine whether P53 directly binds to the HJURP enhancer to regulate gene transcription, we performed ChIP-qPCR in mutp53 and wtp53 breast cancer cells. However, no P53 occupancy at this regions was detected (Supplementary 4D). We applied a discovery P53BLD tool (p53 Binding Loci Database) for identifying the genome-wide binding loci of human P53. P53 ChIP-seq data of breast cancer cell lines (MCF-7, HCC70, BT-549 and MDA-MB-468) was re-mapped to visualize the regions with significant enrichment of P53 binding in the genome (Supplementary 4E). These two results demonstrated no physical association between the P53 and HJURP enhancer chromatin.

The initiation of individual enhancers activation generally requires multiple TFs binding to DNA response elements, which provide a flexible, robust and finely tuned mechanism for regulating gene expression programmes. To explore the underlying mechanism for p53-mediated transcription repression, we sought to identify P53 -interacting proteins. *E2F1* acts upstream of P53, which links the Rb/E2F proliferation pathway and the P53 apoptosis pathway[19]. It has been proposed that P53 and *E2F1* co-ordinately modulate *FOXM1* transcription through an E2F-binding site located within the proximal promoter region[20,21]. To assess whether the *E2F1* and *FOXM1* are involved in the P53-dependent *HJURP* repression, we firstly analysed the expression pattern of *E2F1* and *FOXM1* with *HJURP*. A close positive correlation between the expression pattern of *E2F1* and *FOXM1* with *HJURP* was presented (Fig. 6H). We next determined the involvement of *E2F1* and *FOXM1* in P53-mediated accumulation of *HJURP*. Knock-down of *E2F1* or *FOXM1* significantly suppressed HJURP mRNA and protein expression in mutp53-containing cells (BT-549 and MDA-MB-231). Expression levels of CENP-A, MDM2 and p21 were also reduced upon E2F1 silencing (Fig. 6I - L). Besides, comparable decreased expression of HJURP as well as FOXM1-activated genes (*CCNB1, CDC25B and PLK1*) were detected in MDA-MB-231 cells treated with the FOXM1 inhibitor (FDI6) (Supplementary Fig. 4F). The expression of HJURP and other established transcriptional targets of FOXM1 or E2F1 were also down-regulated upon knockdown of E2F1 or FOXM1(Supplementary Fig. 4G). FDI6 as an inhibitor of FOXM1 binding, specifically down-regulated these FOXM1-activated genes with FOXM1 occupancy confirmed. The binding affinity of FOXM1 to the enhancer region (E1-4) of HJURP was suppressed after a 6 h treatment with the molecule (Supplementary Fig. 4H). Motif enrichment analyses of chromatin-defined enhancer sequences of HJURP identify the sequence-specific motifs (C/TAAACA) of the transcription factor FOXM1 as well as the binding motif of E2F1 (Supplementary Fig. 4I). To further explore the functional consequence of an interaction between 53, FOXM1 and E2F1, we detected the expression of E2F1 and FOXM1 with P53 silencing in MDA-MB-231 cells. Expression of E2F1 and FOXM1 were reduced after deletion of P53 (Fig. 6M). We then measured enhancer luciferase activity in the presence and absence of FOXM1 and E2F1. Suppression of *E2F1* or *FOXM1* repressed the *HJURP* enhancer activity (Fig. 6N). In TNBC cells harboring mutp53, E2F1 and FOXM1 were found to occupy the proximal enhancer region of HJURP, which could be inhibited by the depression of P53 (Fig. 6O). However, we didn't detect an interaction of P53 with E2F1 and FOXM1 (Supplementary Fig. 4J). In summary, these observations supported a direct role of P53 in regulating *HJURP* transcription through association with *E2F1* and *FOXM1*-modulated enhancer.

Increased HJURP **expression correlated with the unfavorable prognostic effect of breast cancer patients**

We next assessed the survival biomarkers value of *HJURP* by an online Kaplan-Meier Plotter, which incorporates microarray data with the prognosis information of breast cancer patients. Breast cancer patients were divided into two groups by auto-selection of best cut-off. There was a significant association of elevated *HJURP* mRNA level with unfavourable prognosis in patients with breast cancer. To determine whether *HJURP* expression status correlates with disease-free and overall survival, we analysed four independent breast cancer datasets, demonstrating that high *HJURP* mRNA level is a prognostic factor for poor survival in all datasets. (Fig. 7A, B).

To further examine whether the poor outcome associated with elevated *HJURP* mRNA levels depend on the promoting effect of *HJURP* in mutp53-subtype cancers, a cohort of 236 breast cancer patients from GEO dataset (GSE3494) with annotated P53 mutation status and information of clinical outcomes was used. We noted an inverse relationship between *HJURP* levels and outcomes of breast patients expressing wild-type, but not mutant, P53 (largely a consequence of the limited number of patients with mutp53 in these last groups). Significant associations were established between *HJURP* and overall survival in breast cancer patients carrying wtp53 (Fig. 7C). No significant prognostic relevance of *HJURP* expression levels with breast cancer patients with mutp53 was identified, which could be caused by the overall activation of *HJURP* in this subtype cancer. Segregating the breast cancer patient cohort into four major molecular subtypes (luminal A, luminal B, HER2-enriched and triple negative/basal-like), a significant association was identified between *HJURP* and clinical outcomes in luminal A/B, but not in basal or HER-2 subtypes. These results showed that increased *HJURP* mRNA levels are related to unfavourable prognosis, especially for tumors carrying wtp53 and luminal-breast cancer (Fig. 7D). Our findings identify *HJURP* acts as a molecular bypass that overcomes the anti-proliferative and pro-apoptotic effects exerted by wtp53 in breast cancer.

Discussion

TNBC is a heterogeneous group with innate aggressive biological characteristics, but lack of effective therapies. With integrated analysis of H3K27ac ChIP-seq combining gene expression profiling, we identified *HJURP* as a specific enhancer-driven transcript in TNBC of functional relevance. Experimentally, *HJURP* mediated increased cell growth, elevated metastatic capacity and protection from apoptosis in TNBC. High *HJURP* expression levels were also associated with poor prognosis, especially for tumors carrying wtp53 and luminal-subtype breast cancer. We further discovered that activation of *HJURP* is associated with P53 mutation status, and high *HJURP* expression is caused by loss-function of wtp53. Accumulation of wtp53 repressed *HJURP* transcription by blocking the recruitment of active enhancer co-factors as BRD4, RNA polymerase II and H3K27ac in non-TNBCs. Of note, in TNBCs with mutp53, knock-down of mutp53 led to decreased *E2F1* and *FOXM1* expression, thus inhibiting *HJURP* enhancer activity and gene transcription.

The histone chaperone *HJURP* mediates *CENP-A* nucleosomes assembly and maintenance at centromeres[13]. To maintain genomic integrity, tight regulation of *HJURP* is necessary to suppress mutagenic potential[22,23]. The oncogenic function of *HJURP* has been reported in the progression of liver cancer, lung cancer, brain cancer, breast cancer, and ovary cancer and elevation of *HJURP* is also strongly correlated with unfavourable prognosis of cancer patients[24–27]. This study further investigated the molecular basis underlying increased *HJURP* expression in TNBCs. Our studies demonstrated that high expression of *HJURP* is due to the loss-function or mutation of wtp53 in TNBCs, in agreement with the previous report[28]. A similar relationship between *HJURP* value and P53 status can be extended to bladder, lung cancers, strong evidence that elevation of *HJURP* in tumors expressing mutant-p53 is not specific to breast cancer but common in other human tumors. Knock-down of wtp53 increases *HJURP* expression,

while Nutlin-3a activation of wtp53 represses *HJURP* expression in multiple cell types, suggesting that wtp53 negatively regulates *HJURP* transcription in breast cancer. Several molecular mechanisms directing repression of P53 target genes have been revealed, either direct recruitment of *p53*, or indirect binding via interaction with co-TFs. Our results further found *E2F1* and *FOXM1* participate in the regulation of mutp53-activated *HJURP* transcription. *FOXM1* and *E2F1* are master transcription factors in human cancer[19]. *E2F1* and *FOXM1* play a possible role in the DNA damage response and drug resistance in breast cancer. P53 represses *FOXM1* transcription through an E2F-binding site located within the proximal FOXM1 promoter region. The loss-function of FOXM1 by P53 contributes to epirubicin resistance of breast cancer [20]. In TNBCs carrying mutp53, knock-down of mutp53 led to deletion of *E2F1* and *FOXM1* expression, with reduced H3K27ac binding affinity and disruption of specific *HJURP*-enhancer, thereby inhibiting *HJURP* transcription. Here, we demonstrated mut*p53* regulate *HJURP* transcription associated with the positive function of *E2F1* and *FOXM1*. Besides, we detected the activation of HJURP in HER2-positive SKBR3 cell, with lower H3K27ac signals within the enhancer region. Theoretically, H3K27ac is a deterministic feature of active enhancers, and there is an enrichment of H3K27Ac among most over-expressed genes. Here, we speculate that H3K27ac alone is not capable of functionally determining enhancer activity and HJURP transcription in SKBR3 cells. The transcription activation of HJURP in SKBR3 cells could be well maintained by the other enhancer features or co-regulators binding to the enriched regions. In breast cancer, the presence of P53 mutation is associated with more aggressive tumors and worse clinical survival, and different approaches have been taken to develop strategies of targeting dysfunctional P53 or restoring P53 functions for cancer treatment. Of note, *HJURP* expression correlated with poor prognosis in breast cancer patients with wtp53 and luminal subtype. These *HJURP*-high expression of subtype-specific breast cancer patients may benefit from targeted treatment strategies.

Tumor suppressor P53 mediates its canonical role as “guardian of the genome” by altering expression of genes to promote cell cycle arrest, apoptosis, cellular senescence and metabolism[29]. wtp53 inactivation or mutp53 caused elevated *HJURP* expression of TNBCs, which would have important clinical implications for tumour development and progression, targeted cancer therapies against oncogenic drivers, both through its function in transcription and its potential for inflicting mutational damage. Previously we used superenhancers screening with active enhancer marker H3K27ac in t(4;14)-translocated multiple myeloma to identify genes related to myeloma cells proliferation. We first demonstrated the aberrant increased expression of superenhancer-driven *HJURP* of t(4;14)-positive myeloma. Oncogenic *HJURP* promoted cell proliferation and abrogated apoptosis, which could be a valuable therapeutic target. Our study collectively identified *HJURP* is regulated through a novel enhancer uniquely present in TNBCs, which is a downstream target gene of P53. Gene expression profiling by transcriptome analysis combined with bioinformatic analyses and mechanistic *in vitro* experiments, suggesting the oncogenic role of *HJURP* in promoting cell proliferation, metastasis, invasion and chemotherapy response. Besides, we also found the Hippo/YAP pathway is relevant in mediating *HJURP* function in affecting cell proliferation and chemotherapy-sensitive in TNBCs, which would be further studied in another research.

P53 functions as a pioneering factor in shaping enhancer activity and key gene such as transcription. Previously research found most of *p53*-bound enhancer elements are located within inaccessible chromatin regions, which may account for the role of the P53 network to function across the diverse chromatin landscapes of various cell types[12]. Here, in wtp53 breast cancer cell, wtp53 may occupy the specific enhancer region of *HJURP* and repress *HJURP* transcription. In loss function of P53 or mutp53 TNBCs, accumulation of active enhancer markers as H3K27ac, BRD4 and RNA POL II was detected in the *HJURP* enhancer sites, followed by the induction of enhancer-driven *HJURP* transcription. P53 could regulate the activity of its target gene as *HJURP*, in part, by modulating chromatin accessibility.

Conclusions

Taken together, we highlight that the P53 regulate *HJURP* transcription by shaping specific enhancer activity in association with co-TFs *E2F1* and *FOXM1* of TNBCs. These studies demonstrated specific transcriptional addictions in TNBCs pathobiology and identified *HJURP* as a potential biomarker and therapeutic target.

Declarations

Significance statement:

HJURP is an enhancer-driven oncogene and potentiates TNBC proliferation and invasion;

P53 regulates *HJURP* transcription through *E2F1* in enhancer chromatin, and *FOXM1* mediates the interaction within this motif.

Ethics approval and consent to participate

The experimental protocol was established, according to the ethical guidelines of the Helsinki Declaration and was approved by the Human Ethics Committee of Zhejiang University. Written informed consent was obtained from individual or guardian participants.

Consent for publication

Not applicable

Availability of supporting data

Not applicable

Conflict of Interest statement

The authors declare that they have no competing interests

Acknowledgements

Funding

This study is supported by National Natural Science Foundation of China (No. 82000212, 82102814, 82100161), Natural Science Foundation of Zhejiang Province (LQ21H160022, LQ22H160053), Medical Health Science and Technology Project of Zhejiang Provincial Health Commission (2021RC003).

Authors' contributions

Y.J., Y.C. and M.C. performed experimental work; J.Z., W.J.C., and J.Z. analyzed data; M.X., Q.J. and M.H. wrote manuscript; H. X., K.C. contributed to sample preparation. Y.J., Y.C. and M.C. contributed equally to this work; J. R., L.W., and P.S. designed and supervised the study. All authors provided critical feedback and helped shape the research, analysis and manuscript.

References

1. Sung H, Ferlay J, Siegel R L, et al. Global cancer statistics 2020: GLOBOCAN estimates of incidence and mortality worldwide for 36 cancers in 185 countries[J]. CA: a cancer journal for clinicians, 2021, 71(3): 209-249.
2. Koboldt D, Fulton R, McLellan M, et al. Comprehensive molecular portraits of human breast tumours[J]. Nature, 2012, 490(7418): 61-70.
3. Sur I, Taipale J. The role of enhancers in cancer. Nat Rev Cancer. 2016 Aug;16(8):483-93.
4. Dong J, Li J, Li Y, Ma Z, Yu Y, Wang CY. Transcriptional super-enhancers control cancer stemness and metastasis genes in squamous cell carcinoma. Nat Commun. 2021 Jun 25;12(1):3974.
5. Huang, H., Hu, J., Maryam, A., et al. Defining super-enhancer landscape in triple-negative breast cancer by multiomic profiling. Nature communications, 2021, 12(1), 2242.
6. van Groningen T, Koster J, Valentijn LJ, et al. Neuroblastoma is composed of two super-enhancer-associated differentiation states. Nat Genet. 2017;49(8):1261-1266.
7. Riley T, Sontag E, Chen P, Levine A. Transcriptional control of human p53-regulated genes. Nat Rev Mol Cell Biol. 2008 May;9(5):402-12.
8. Coles, C., Condie, A., Chetty, U., et al. p53 mutations in breast cancer. *Cancer research*, 1992, *52*(19), 5291-5298.
9. Wellenstein M D, Coffelt S B, Duits D E M, et al. Loss of p53 triggers WNT-dependent systemic inflammation to drive breast cancer metastasis[J]. Nature, 2019, 572(7770): 538-542.
10. Girardini J E, Napoli M, Piazza S, et al. A Pin1/mutant p53 axis promotes aggressiveness in breast cancer[J]. Cancer cell, 2011, 20(1): 79-91.
11. Melo C A, Drost J, Wijchers P J, et al. eRNAs are required for p53-dependent enhancer activity and gene transcription[J]. Molecular cell, 2013, 49(3): 524-535.
12. Younger S T, Kenzelmann-Broz D, Jung H, et al. Integrative genomic analysis reveals widespread enhancer regulation by p53 in response to DNA damage[J]. Nucleic acids research, 2015, 43(9):

4447-4462.

13. Shuaib M, Ouararhni K, Dimitrov S, et al. HJURP binds CENP-A via a highly conserved N-terminal domain and mediates its deposition at centromeres[J]. Proceedings of the National Academy of Sciences, 2010, 107(4): 1349-1354.
14. Andronov L, Ouararhni K, Stoll I, et al. CENP-A nucleosome clusters form rosette-like structures around HJURP during G1[J]. Nature communications, 2019, 10(1): 1-8.
15. Hu Z, Huang G, Sadanandam A, et al. The expression level of HJURP has an independent prognostic impact and predicts the sensitivity to radiotherapy in breast cancer[J]. Breast cancer research, 2010, 12(2): 1-15.
16. de Oca R M, Gurard-Levin Z A, Berger F, et al. The histone chaperone HJURP is a new independent prognostic marker for luminal A breast carcinoma[J]. Molecular oncology, 2015, 9(3): 657-674.
17. Jia Y, Zhou J, Tan TK, Chung TH, Chen Y, Chooi JY, Sanda T, Fullwood MJ, Xiong S, Toh SHM, Balan K, Wong RWJ, Lim JSL, Zhang E, Cai Z, Shen P, Chng WJ. Super Enhancer-Mediated Upregulation of HJURP Promotes Growth and Survival of t(4;14)-Positive Multiple Myeloma. Cancer Res. 2022 Feb 1;82(3):406-418.
18. Filipescu D, Naughtin M, Podsypanina K, Lejour V, Wilson L, Gurard-Levin ZA, Orsi GA, Simeonova I, Toufektchan E, Attardi LD, Toledo F. Essential role for centromeric factors following p53 loss and oncogenic transformation. Genes & development. 2017 Mar 1;31(5):463-80.
19. Rogoff HA, Pickering MT, Debatis ME, Jones S, Kowalik TF. E2F1 induces phosphorylation of p53 that is coincident with p53 accumulation and apoptosis. Molecular and cellular biology. 2002 Aug 1;22(15):5308-18.
20. Millour J, de Olano N, Horimoto Y, Monteiro LJ, Langer JK, Aligue R, Hajji N, Lam EW. ATM and p53 regulate FOXM1 expression via E2F in breast cancer epirubicin treatment and resistance. Molecular cancer therapeutics. 2011 Jun 1;10(6):1046-58.
21. Fischer M, Grossmann P, Padi M, DeCaprio JA. Integration of TP53, DREAM, MMB-FOXM1 and RB-E2F target gene analyses identifies cell cycle gene regulatory networks. Nucleic acids research. 2016 Jul 27;44(13):6070-86.
22. Foltz DR, Jansen LE, Bailey AO, Yates III JR, Bassett EA, Wood S, Black BE, Cleveland DW. Centromere-specific assembly of CENP-a nucleosomes is mediated by HJURP. Cell. 2009 May 1;137(3):472-84.
23. Tachiwana H, Müller S, Blümer J, Klare K, Musacchio A, Almouzni G. HJURP involvement in de novo CenH3CENP-A and CENP-C recruitment. Cell reports. 2015 Apr 7;11(1):22-32.
24. Kato T, Sato N, Hayama S, Yamabuki T, Ito T, Miyamoto M, Kondo S, Nakamura Y, Daigo Y. Activation of Holliday junction–recognizing protein involved in the chromosomal stability and immortality of cancer cells. Cancer research. 2007 Sep 15;67(18):8544-53.
25. Wei Y, Ouyang GL, Yao WX, Zhu YJ, Li X, Huang LX, Yang XW, Jiang WJ. Knock-down of HJURP inhibits non-small cell lung cancer cell proliferation, migration, and invasion by repressing Wnt/β-catenin signaling. Eur Rev Med Pharmacol Sci. 2019 May 1;23(9):3847-56.

26. Chen T, Huang H, Zhou Y, Geng L, Shen T, Yin S, Zhou L, Zheng S. HJURP promotes hepatocellular carcinoma proliferation by destabilizing p21 via the MAPK/ERK1/2 and AKT/GSK3β signaling pathways. Journal of Experimental & Clinical Cancer Research. 2018 Dec;37(1):1-4.
27. Lai W, Zhu W, Xiao C, Li X, Wang Y, Han Y, Zheng J, Li Y, Li M, Wen X. HJURP promotes proliferation in prostate cancer cells through increasing CDKN1A degradation via the GSK3β/JNK signaling pathway. Cell death & disease. 2021 Jun 7;12(6):1-2.
28. Filipescu D, Naughtin M, Podsypanina K, Lejour V, Wilson L, Gurard-Levin ZA, Orsi GA, Simeonova I, Toufektchan E, Attardi LD, Toledo F. Essential role for centromeric factors following p53 loss and oncogenic transformation. Genes & development. 2017 Mar 1;31(5):463-80.
29. Levine AJ, Momand J, Finlay CA. The p53 tumour suppressor gene. Nature. 1991 Jun;351(6326):453-6.

Tables

Tables are available in the Supplementary Files section.

Figures

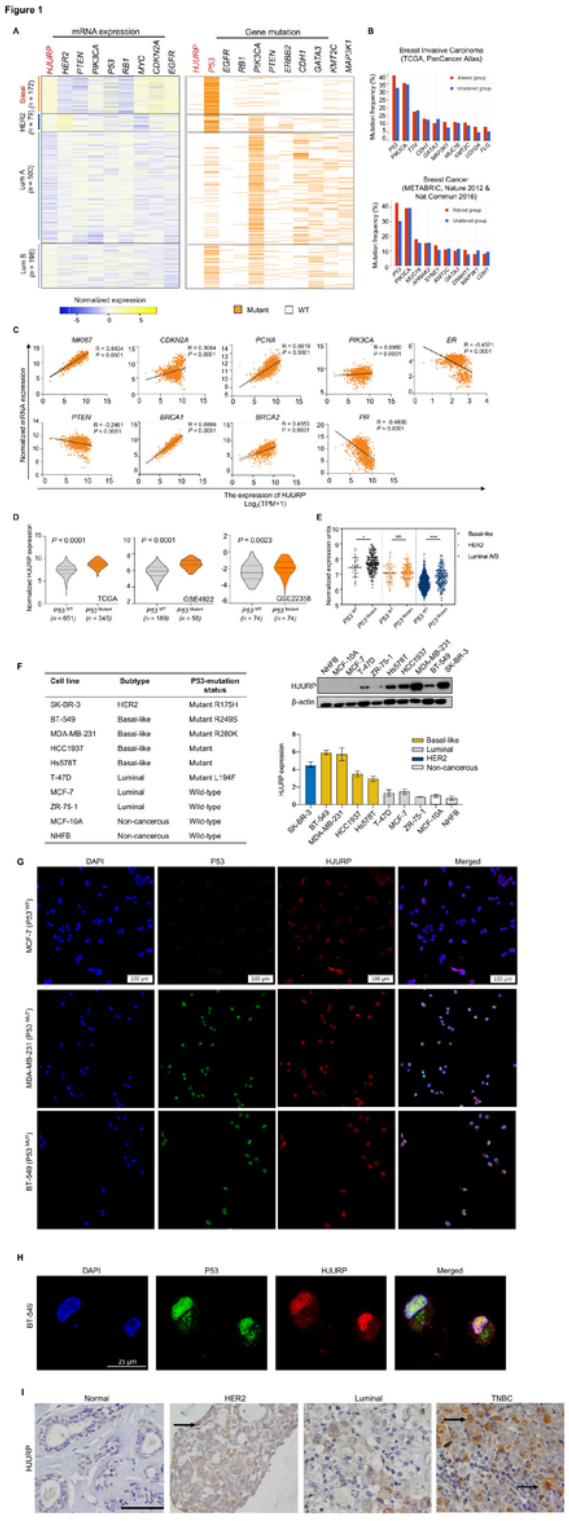

Figure 1

Expression and genomic alteration of *HJURP* in breast cancer

A. Analysis of breast tumor samples from the TCGA to determine the co-occurrence of high *HJURP* expression with oncogenic mutations in the intrinsic molecular subtypes of breast cancer. High *HJURP* expression was defined as a microarray z-score of > 2.0. **B.** Frequency of common somatic mutations

and distribution of these mutations of breast cancer data sets (TCGA and METABRIC). The method identified P53 mutation status is highly correlated with drastic changes in the expression of *HJURP* (z-score ± 2.0), across tumor samples. **C**. Correlation among genes potentially important in tumorigenesis and cancer-specific survival genes with *HJURP* in cancer genomics data. Expression correlated over- and under-expressed genes with $P < 0.05$ (Fisher's exact test). **D**. Comparison of *HJURP* mRNA expression between P53 wild-type and P53-mutant breast cancer patient samples (TCGA, GSE4922 and GSE22358). The scale for *HJURP*expression is log2-median-centered ratio. Error bars represent a range of minimum to maximum log2-median-centered HJURP expression levels. The box encompasses the upper and lower quartiles. The central line represents the median. **E**. Comparison of *HJURP* mRNA expression between P53 wild-type and P53-mutant in the intrinsic molecular subtypes of breast cancer samples. **F.** Western blotting and qRT-PCR analysis of *HJURP* expression in a panel of breast cell lines with known P53 mutation status. GAPDH was used as a loading control. **G.** HJURP (red) and P53 protein (green) in MCF-7 (wtp53), MDA-MB-231 (mutp53) and BT-549 (mutp53) cells was determined with immunofluorescence staining with DAPI (blue) counterstaining. Scale bars, 100 μM. **H**. Immunofluorescence assay detected that HJURP protein (red) mainly localized to the nucleoplasm & nuclear in the mutp53 BT-549 cell. DNA (blue) was stained with DAPI. Scale bars, 20 μM. **I.** Representative images of tumor sections breast TMA stained for HJURP of intrinsic molecular subtypes of breast cancer. Magnification: 20×, Scale bar: 100 μM. *Statistical significance of P-value < 0.05. Error bars represent ± SE.

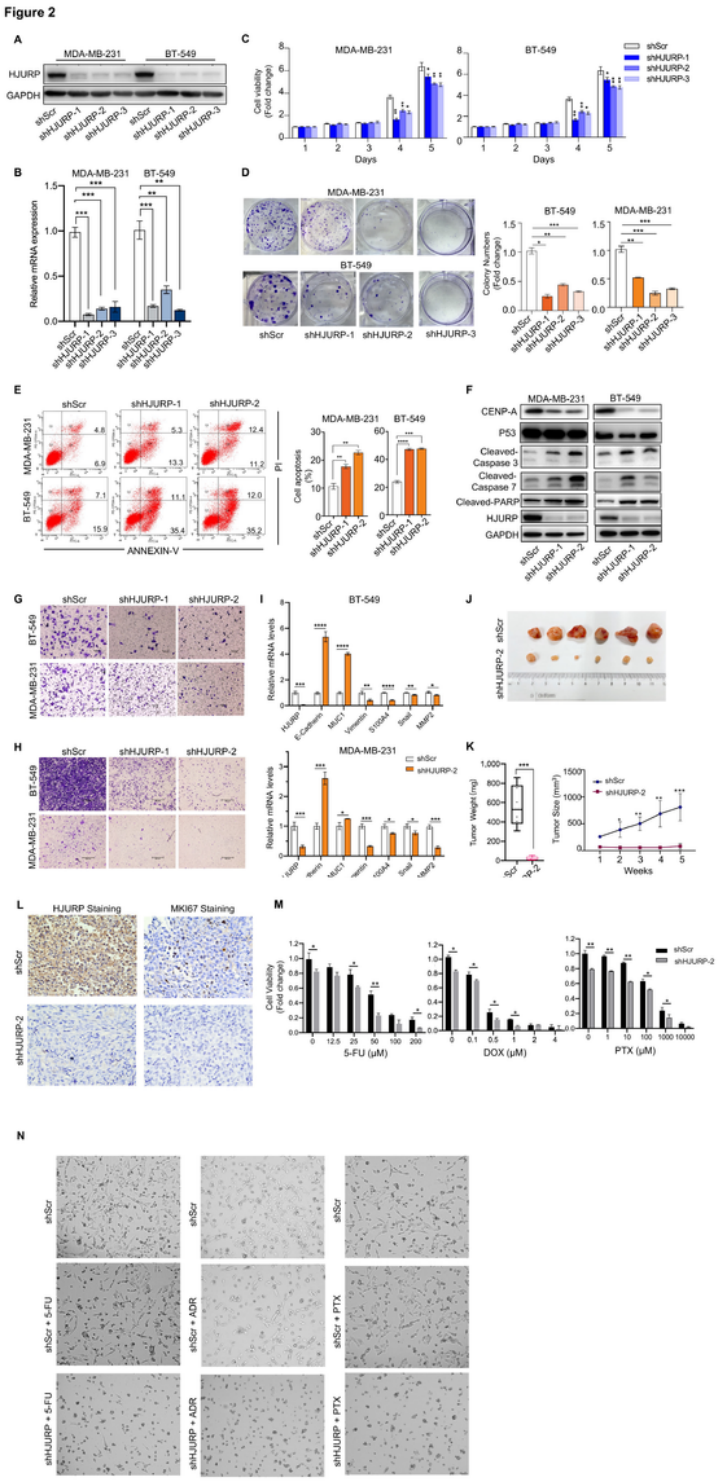

Figure 2

HJURP knock-down impaired breast cancer cell proliferation and migration harboring P53 disruption.

A, B. Expression levels of HJURP protein (A) and mRNA (B) were detected upon HJURP shRNA transfection or the control vector in MDA-MB-231 and BT-549 cells. **C.** Proliferation of MDA-MB-231 and BT-549 cells were significantly inhibited upon *HJURP* silencing. The cell proliferation was tested every 24

h using MTT assays. **D**. Representative images of colony formation assays of the MDA-MB-231 and BT-549 cell lines. *HJURP* silencing decreased the colony-forming efficiencies in both cell lines. **E**. MDA-MB-231 and BT-549 cells were transfected with the CTRL or HJURP shRNA vector for 72 hours. Examination for apoptotic was performed by annexin V staining and flow cytometry. The percentage of apoptotic cells was represented in a bar diagram from three independent experiments. **F**. MDA-MB-231 and BT-549 cells were transfected with the CTRL or HJURP shRNA vector for 48 hours. Examination for apoptotic-marker (cleaved-Caspase 3, cleaved-Caspase 7 and cleaved-PARP) was analyzed by western-blot. Detection of GAPDH protein was used as an internal loading control. **G**, **H**. The cell migration (G) and invasion (H) abilities were measured after transfection with shHJURP or shScr in BT-549 and MDA-MB-231 cells. Cells migrating and invading the lower Transwell chambers were counted (magnification, ×200). **I.** Representative western blot images HJURP, E-Cadherin, MUC1, Vimentin, S100A4, Snail and MMP2 were analyzed with GAPDH as an internal control at 48 h after transfection with HJURP siRNA or NC in BT-549 and MDA-MB-231 cells. **J, K**. Representative tumor grafts are shown, which were grown in nude mice injected with MDA-MB-231/shScr and MDA-MB231/shHJURP cells. Tumor weight and tumor volume were compared between the HJURP-silencing and control groups. The tumor volume was calculated using the following equation: V = (width2 × length)/2. **L.** Representative images of HJURP and KI67 staining are presented in each group of nude mice using immunohistochemistry analysis. **M**. Drug sensitivity test for 5-FU, Dox and PTX in BT-549 cells infected with shScr and HJURP shRNA. Cells were treated with various indicated concentrations of 5-FU, Dox and PTX for 48 h, cell viability upon drug treatment was analyzed by an MTT assay. **N**. Morphology in BT-549 cell aggressive basal-like upon 5-FU, Dox and PTX treatment infected with NC and HJURP shRNA. * $P < 0.05$, ** $P < 0.01$ in a comparison between cells transfected with control nontargeting (shScr) and HJURP shRNA.

Figure 3

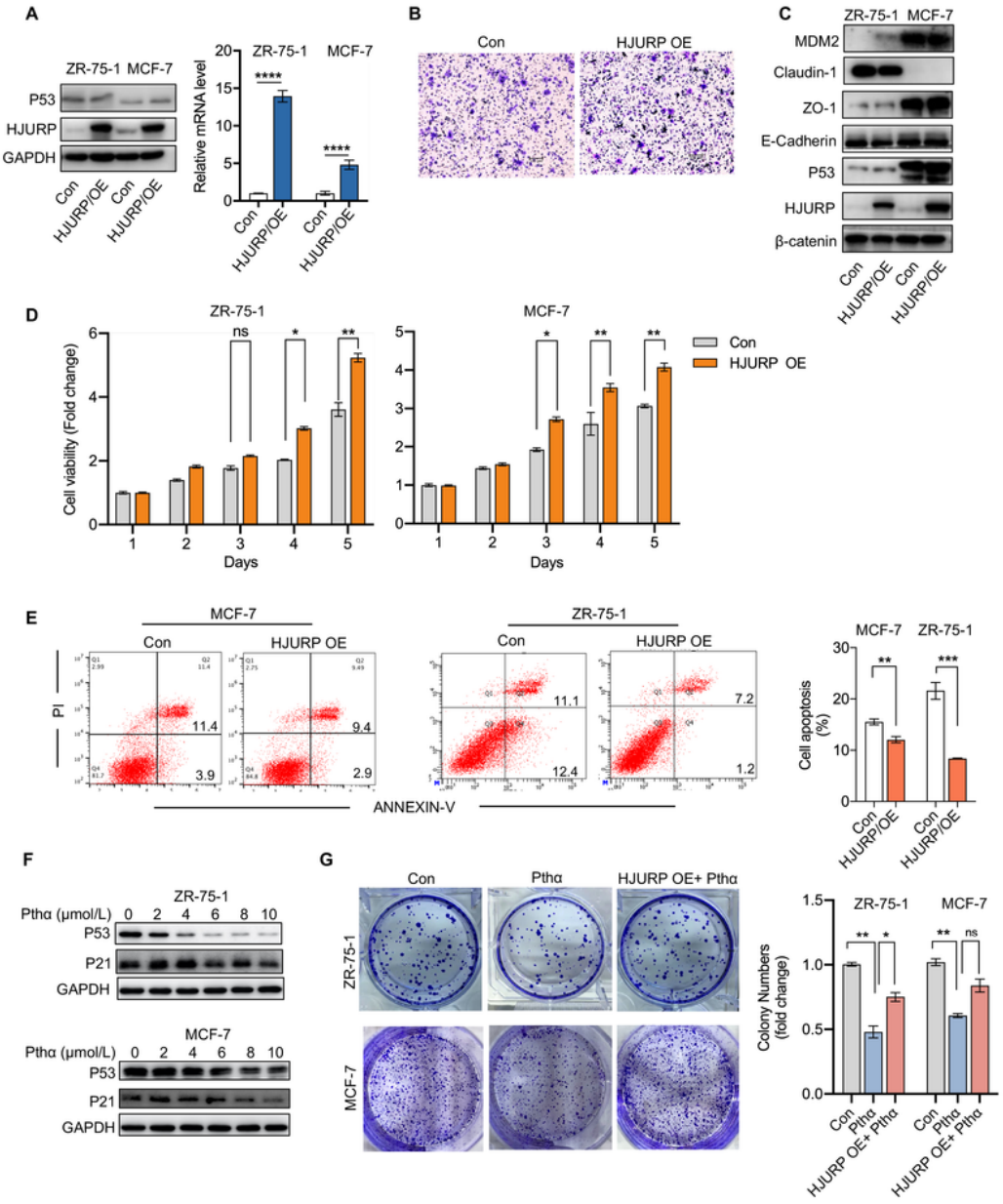

Figure 3

***HJURP* promoted cell proliferation and suppressed apoptosis dependent on loss function of** P53**.**

A. Expression levels of HJURP protein (A) and mRNA (B) expression of HJURP and p53 in the HJURP-overexpressing cell lines ZR-75-1 and MCF-7 and the negative controls. GAPDH served as the endogenous control. **B**. The cell migration abilities were measured by Transwell migration assays after transfection

with CTRL or HJURP overexpression vector in MCF-7 cells. **C**. Representative western blot images HJURP, P53, E-cadherin, ZO-1, Claudin-1 and MDM2 were analyzed with GAPDH as an internal control at 48 h after transfection with CTRL or *HJURP*overexpression vector. **D**. Proliferation of ZR-75-1 and MCF-7 cells were significantly increased upon *HJURP* overexpression. The cell proliferation was tested every 24 h using MTT assays. **E**. ZR-75-1 and MCF-7 cells were transfected with the CTRL or HJURP overexpression vector for 48 hours. Examination for apoptotic was performed by annexin V staining and flow cytometry. The percentage of apoptotic cells was represented in a bar diagram from three independent experiments. **F**. Expression levels of P53 and p21 protein expression in MCF-7 and ZR-75-1 cells upon indicated concentration of Pthα treatment. GAPDH served as the endogenous control. **G**. Representative images of colony formation assays of the MCF-7 and ZR-75-1 cell lines infected with *HJURP*overexpression vector or treatment with Pthα.

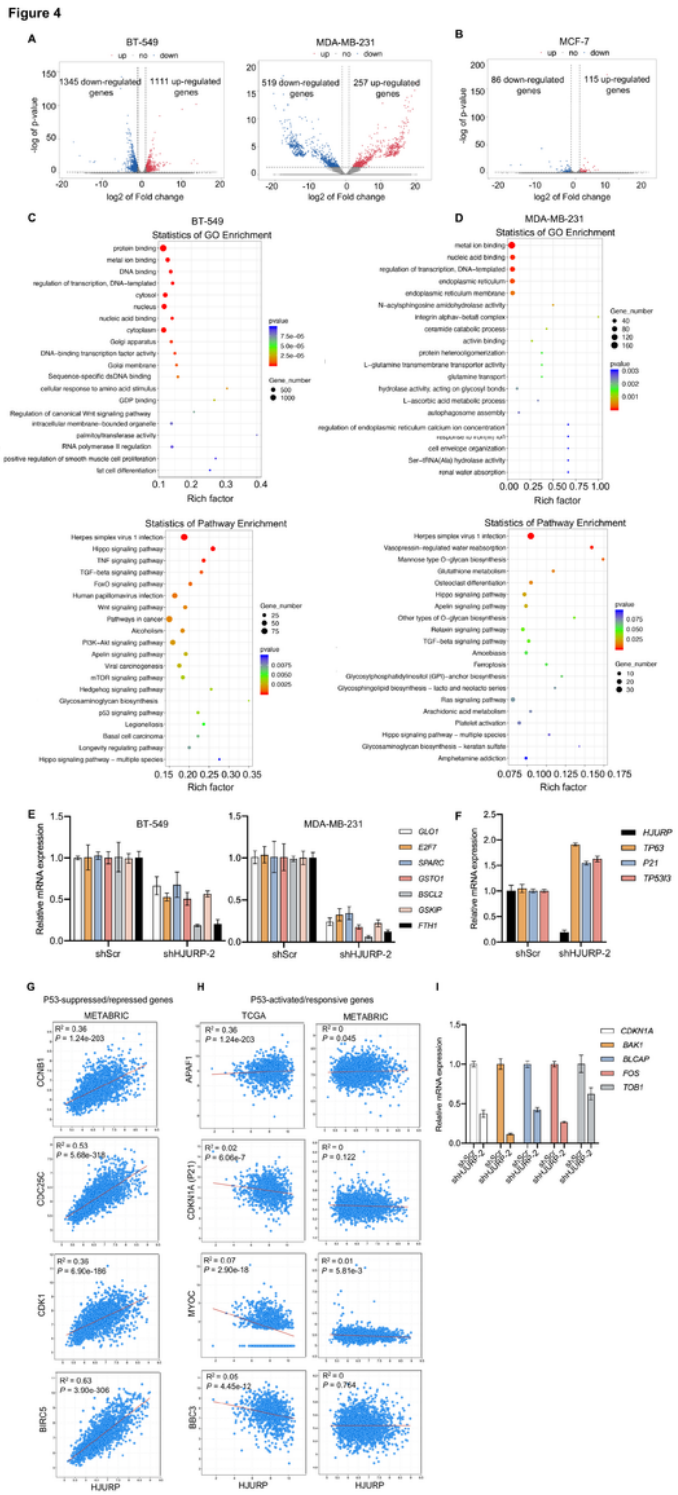

Figure 4

Identification of gene expression signature of *HJURP* induction

A. Volcano plot of up- and down regulated genes (*P*-value <0.05, fold change >2) in shHJURP-infected BT-549 and MDA-MB-231 cells compared with control nontargeting (NC). **B**. Volcano plot of up- and down regulated genes (*P*-value <0.05, fold change >2) in *HJURP* overexpression vector-infected MCF-7 cells

compared with control nontargeting (NC). The red dots represent significantly up-regulated genes, the green dots represent significantly downregulated genes , and the black dots represent insignificant differentially expressed genes. **C, D**. Go and KEGG pathway enrichment of differentially expressed genes in shHJURP-infected BT-549 (C) and MDA-MB-231 (D) cells compared with control nontargeting (NC). Advanced bubble chart shows enrichment of differentially expressed genes in Go term and signaling pathways. The x-axis represents rich factor (rich factor = number of DEG enriched in the pathway/number of all genes in the background gene set). The y-axis represents the enriched pathway. Color represents enrichment significance, and size of the bubble represents the number of DEG enriched in the pathway. **E, F**. qRT-PCR validation of representative downregulated and up-regulated genes upon *HJURP*deletion. Expression levels were normalized to GAPDH gene. The bars represent standard errors from three replicates, and statistical tests were conducted using t test for multiple comparisons. Values on the bars followed by different letters are significantly different at $P < 0.05$. **G, H.** Correlation analysis of normalized expression of validated reported P53 target repressed (G) or activated genes (H) versus the average expression of *HJURP*. R: correlation coefficient. **I.** The mRNA levels of selected P53-repressed genes (*CDKN1A, BAK1, BLCAP, FOS, TOB1*) upon *HJURP* silencing in BT-549 cells.

Figure 5

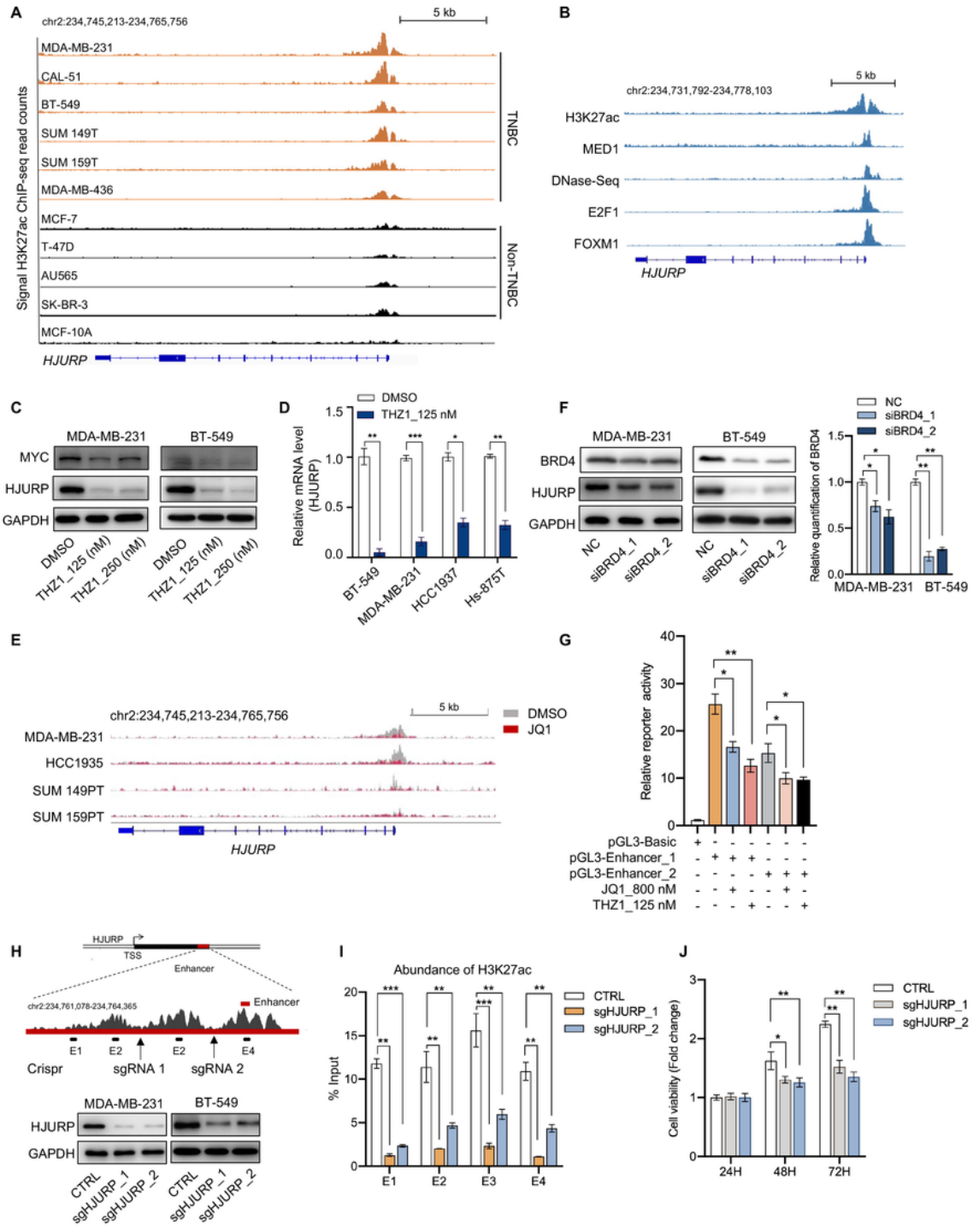

Figure 5

Repression of enhancer activity inhibited *HJURP* transcription and phenocopied *HJURP* silencing

A. ChIP-seq data tracks showing the abundance of H3K27ac within HJURP loci and its enhancer region of TNBC (MDA-MB-231, CAL-51, BT-549, SUM 149T, SUM159T and MDA-MB-436), non-TNBC samples (MCF-7, T-74D, AU566, SK-BR-3) and normal breast non-tumorigenic epithelial cell line (MCF-10A). Public

H3K27ac ChIP-Seq data were collected and visualized by the ChIP-Atlas database (https://chip-atlas.org/). **B.** ChIP-seq data tracks showing the enrichment of H3K27ac, MED1, DNase-Seq, E2F1 and FOXM1 at the HJURP enhancer region. **C**. MDA-MB-231 and BT-549 cells were treated DMSO or THZ1 at a concentration of 125 nM and 250 nM for 24 h, and HJURP expression level was analyzed by western blotting. GAPDH was used as a loading control. **D**. qRT-PCR validation of HJURP expression upon THZ1 treatment in BT-549, MDA-MB231, HCC1937 and Hs-875T. Expression levels were normalized to GAPDH gene. The bars represent standard errors from three replicates, and statistical tests were conducted using t's test for multiple comparisons. Values on the bars followed by different letters are significantly different at $P<0.05$. **E**. ChIP-seq occupancy profiles of BRD4 at the HJURP locus following a 2-hr treatment with DMSO or 500 nM JQ1. **F**. Protein expression levels of HJURP in BT-549, MDA-MB231cells upon depression of BRD4 expression by two individual siRNAs (siBRD4_1 and siBRD4_2) or transfected with the control vector (NC). **G**. Separate fragments of enhancer regions (pGL3-Enhancer_1 and pGL3-Enhancer_2) were subcloned upstream of the luciferase reporter gene. Dual-luciferase reporter assays examining reporter activities 72 hours post-transfection treated with 800 nM JQ1 or 125 nM THZ1 for 24 hours in BT-549 cells. Firefly luciferase activity was measured and normalized to renilla luciferase to control cell number and transfection efficiency, and expressed as a ratio relative to activity of the control enhancer construct. **H**. A schematic diagram of the sgRNA directed dCas9-KRAB transcription repression system, and two sgRNAs designed to target specific sites of the enhancer region of *HJURP*. Protein expression levels of HJURP in BT-549 and MDA-MB231cells cells upon depression of enhancer activity by two individual sgRNAs (sgHJURP_1 and sgHJURP_2) or transfected with the control vector (CTRL). **I**. ChIP-qPCR analysis of H3K27ac at constituent enhancers (E1-E4) in BT-549 cells following depression of *HJURP* enhancer region (sgHJURP_1 and sgHJURP_2) or transfected with the control vector (CTRL). **J**. Cell growth assay after depression of *HJURP* enhancer region or transfected with the control vector (CTRL) for 24, 48, 72 hours in BT-549 cells.

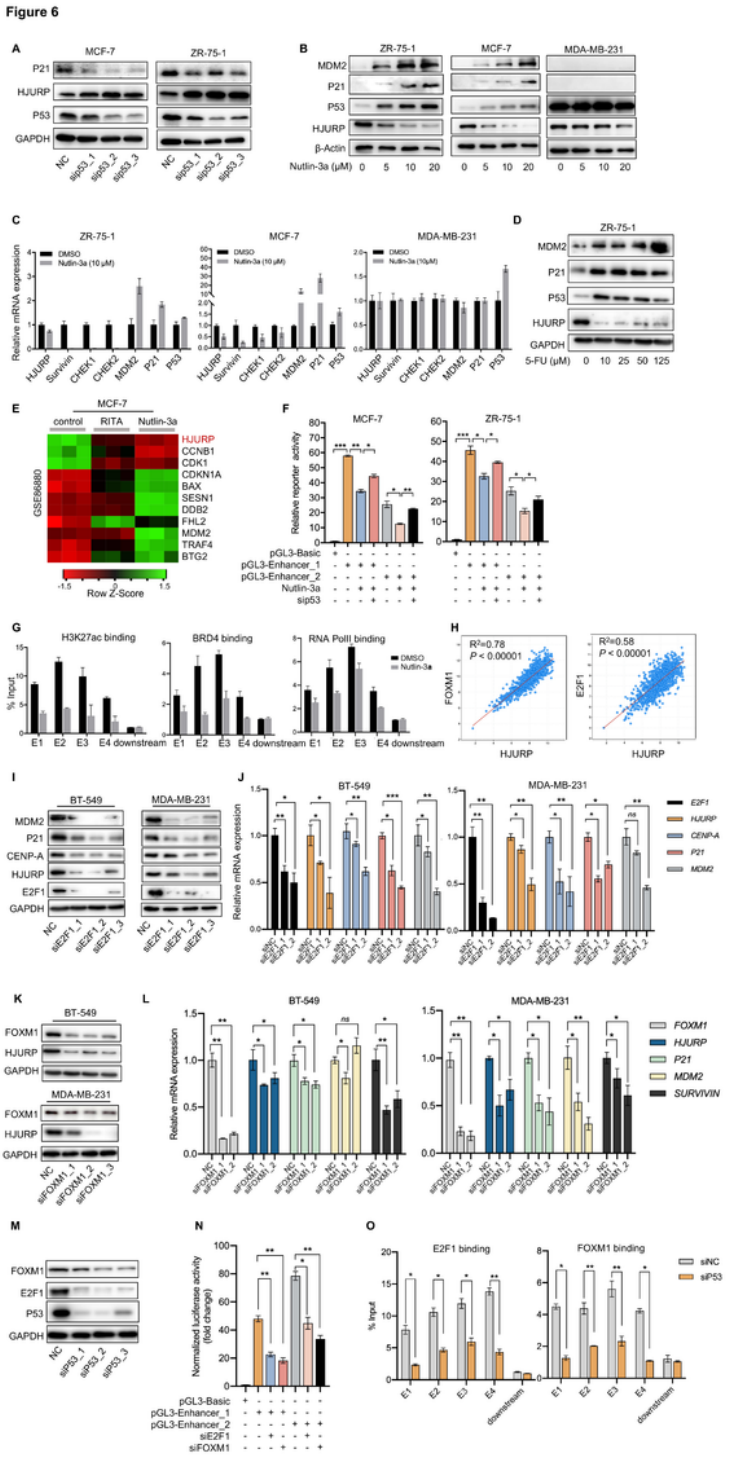

Figure 6

P53/FOXM1/E2F1-axis co-regulated *HJURP* expression

A. The protein expression levels of p21, HJURP and P53 following transfection with three different pairs of P53 siRNA (siP53_1, siP53_2 and siP53_3) or the negative control siRNA (NC) in MCF-7 and ZR-75-1 cells. GAPDH was measured as the loading control. **B**. ZR-75-1, MCF-7 and MDA-MB-231 cells were

treated with DMSO or Nutlin-3a (5, 10, 20 μM) for 24 hours. Then cells were harvested and protein was extracted for Western blot analysis of the indicated markers. **C.** ZR-75-1, MCF-7 and MDA-MB-231 cells were treated with DMSO or 10 μM Nutlin-3a for 24 hours. mRNA levels of HJURP, Survivin, CHEK1, CHEK2, MDM2, p21 and P53 were measured using qRT-PCR. Relative fold changes for the Nutlin-3a-treated samples are displayed as compared to the respective control. Values are presented as the mean ± S.E. **D**. ZR-75-1 cells were treated with DMSO or 5-Fu (10, 25, 50, 125 μM) for 24 hours. Then cells were harvested and protein was extracted for Western blot analysis of HJURP, P53, FOXM1, p21 and MDM2. **E.** A heat map is shown for the differentially expressed genes identified by RNA-seq from MCF-7 untreated or treated with RITA or Nutlin-3a for 24 hours. Up-regulated genes are shown in red, and downregulated genes are shown in green. The scale for the heat map is shown in the bottom panel. **F**. Dual-luciferase reporter assays examining reporter activities 72 hours post-transfection treated with 10 μM Nutlin-3a or P53 silencing for 24 hours in MCF-7 and ZR-75-1 cells. Firefly luciferase activity was measured and normalized to renilla luciferase to control cell number and transfection efficiency, and expressed as a ratio relative to activity of the control enhancer construct. **G**. Abundance of H3K27ac, BRD4 and RNA polymerase II at constituent enhancers (E1-E4) of *HJURP* in BT-549 cells. **H**. Correlation analysis of normalized expression of *FOXM1* or *E2F1*versus the average expression of *HJURP*. R: correlation coefficient. **I**. The protein expression levels of E2F1, HJURP, CENP-A, p21 and MDM2 following transfection with three different pairs of E2F1 siRNA (siE2F1_1, siE2F1_2 and siE2F1_3) or the negative control siRNA (NC) in BT-549 and MDA-MB-231 cells. GAPDH was measured as the loading control. **J**. qRT-PCR analysis of indicated markers (*E2F1, HJURP, CENP-A, p21* and *MDM2*) from BT-549 and MDA-MB-231 cells infected with *E2F1* siRNA or control nontargeting (NC) for 24 hr. **K**. The protein expression levels of FOXM1 and HJURP following transfection with three different pairs of *FOXM1* siRNA (siFOXM1_1, siFOXM1_2 and siFOXM1_3) or the negative control siRNA (NC) in BT-549 and MDA-MB-231 cells. **L**. qRT-PCR analysis of indicated markers (*FOXM1, HJURP, P21, MDM2 and Survivin*) from BT-549 and MDA-MB-231 cells infected with FOXM1 siRNA or control nontargeting (NC) for 24 hr. **M**. The protein expression levels of FOXM1, E2F1 and P53 following transfection with three different pairs of P53 siRNA or the negative control siRNA (NC) in BT-549 cells. **N**. Dual-luciferase reporter assays examining reporter activities 72 hours post-transfection for *E2F1* or *FOXM1*silencing for 24 hours in BT-549 cells. **O**. ChIP-qPCR analysis of E2F1 and FOXM1 binding at constituent enhancers (E1-E4) in BT-549 cells following deletion of P53 expression or transfected with the control vector (siNC).

Figure 7.

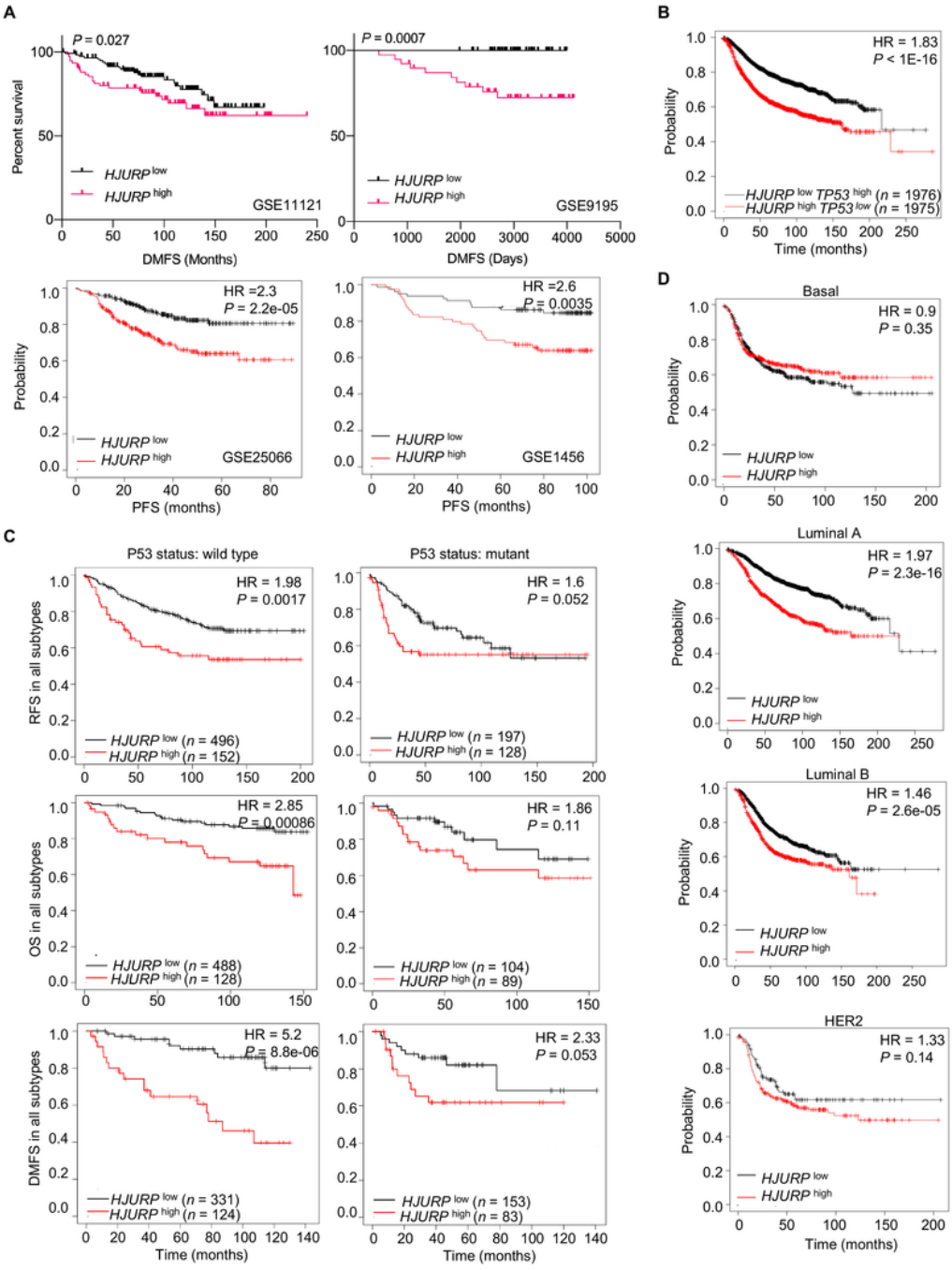

Figure 7

HJURP expression levels correlated negatively with breast cancer patient survival harbouring wild-type, but not mutant, P53 alleles.

A. Kaplan–Meier plot depicting the effect of *HJURP*expression levels on distant metastasis free survival (DMFS) and progression-free survival (PFS) in breast cancer patients. **B**. Kaplan-Meier curves of overall

survival according to the combination of *HJURP* and P53 expression levels. **C.** Prognostic implications of *HJURP* expression profiles in breast cancer patients carrying wtp53 or with P53 mutation, separately. **D**. Predicted survival curves for the different molecular subtypes of breast cancer based on *HJURP* expression profiles. Kaplan-Meier survival curves were compared by Log-rank The P-value noted is derived from a log-rank test.

Supplementary Files

This is a list of supplementary files associated with this preprint. Click to download.

- Suppl.Figure1.jpg
- Suppl.Figure2.jpg
- Suppl.Figure3.jpg
- Suppl.Figure4.jpg
- Table1.jpg
- Table2.jpg